Biogeosciences Discuss., 10, 16173–16211, 2013
www.biogeosciences-discuss.net/10/16173/2013/
doi:10.5194/bgd-10-16173-2013

Biogeosciences
Discussions
Open Access

Ocean-atmosphere exchange of organic carbon and CO_2 in the Antarctic Peninsula – physical and biological controls

S. Ruiz-Halpern[1,8], M. L. Calleja[2], J. Dachs[3], S. Del Vento[3,4], M. Pastor[5], M. Palmer[1], S. Agustí[1,6], and C. M. Duarte[1,7]

[1]Instituto Mediterráneo de Estudios Avanzados (IMEDEA), Consejo Superior de Investigaciones Científicas-Universitat de les Illes Balears (CSIC-UIB), Esporles, I. Balears, Spain
[2]Instituto Andaluz de Ciencias de la Tierra (IACT), Consejo Superior de Investigaciones Científicas – Universidad de Granada (CSIC-UGR), Avda. de las Palmeras 4, 18100 Armilla, Granada, Andalucía, Spain
[3]Instituto de Diagnóstico Ambienal y Estudios del Agua (IDAEA), Consejo Superior de Investigaciones Científicas (CSIC), Barcelona, Cataluña, Spain
[4]Lancaster Environment Centre, Lancaster University, Lancaster, LA1 4YQ, UK
[5]Departamento de Acústica y Geofísica Unidad de Tecnología Marina-Consejo Superior de Investigaciones Científicas (UTM-CSIC), Barcelona, Catalunya, Spain
[6]The UWA Oceans Institute and School of Plant Biology, University of Western Australia, 35 Stirling Highway, Crawley 6009, Australia

[7]The UWA Oceans Institute, University of Western Australia, 35 Stirling Highway, Crawley 6009, Australia
[8]Centre for Coastal Biogeochemistry, School of Environment, Science and Engineering, Southern Cross University, Lismore, New South Wales, Australia

Received: 28 August 2013 – Accepted: 28 September 2013 – Published: 21 October 2013

Correspondence to: S. Ruiz-Halpern (sergio.ruiz-halpern@scu.edu.au)

Published by Copernicus Publications on behalf of the European Geosciences Union.

Title Page
Abstract | Introduction
Conclusions | References
Tables | Figures
◄ | ►
◄ | ►
Back | Close
Full Screen / Esc
Printer-friendly Version
Interactive Discussion

Abstract

Exchangeable organic carbon (OC) dynamics and CO_2 fluxes in the Antarctic Peninsula region during austral summer are highly variable. By stations, the region is a weak source of CO_2 to the atmosphere, however, continuous records of CO_2 revealed this area as a weak sink. OC fluxes are also in both directions but generally towards the ocean and much higher than CO_2 fluxes, sometimes by a factor of 10. Surface exchangeable dissolved organic carbon (EDOC) measurements had a $43 \pm 3\,\mu\mathrm{mol\,C\,L^{-1}}$ overall mean, while the gaseous organic carbon equilibrated in water as given by the Henry's Law constant (H') resulted in (GOC H'^{-1}) concentrations of $46 \pm 3\,\mu\mathrm{mol\,C\,L^{-1}}$. EDOC represents around 66 % of surface dissolved organic carbon (DOC) in Antarctic waters. There is a tendency towards low partial pressures of CO_2 in waters with high Chlorophyll *a* (Chl *a*) content and high fCO_2 in areas with high krill densities. However, such relationships were not found for EDOC. Depth profiles of EDOC were also quite variable and followed Chl *a* profiles, but only in some instances, while diel cycles of EDOC revealed two distinct peaks around midday and middle of the short austral dark period concurrent with solar radiation maxima and krill night migration patterns. However, there was no evident diel pattern for GOC H'^{-1}. The pool of exchangeable OC reveals itself as an important compartment of the carbon budget in the Antarctic Peninsula and adds to previous studies highlighting its importance in the redistribution of carbon in marine environments.

1 Introduction

The ocean and the atmosphere exchange momentum, heat, gas, and materials across an area of 361 million km^2, these interactions playing a major role in the dynamics of the Earth's System (Siedler et al., 2001). Gas exchanges play a key role in climate regulation, as the ocean has already absorbed a large fraction of anthropogenically produced CO_2 (Sabine et al., 2004), the major green house gas (ghg) contributing to global warming. However, the ocean acts as a source of other ghgs, such as methane (Judd et al., 2002) and dimethyl sulfide (DMS) (Charlson et al., 1987; Ayers and Gillett, 2000). The ocean and the atmosphere also exchange a wide variety of volatile and semivolatile organic compounds (VOCs and SOCs), although there is still a lack of comphehensive assessment of the magnitude of these fluxes.

Goldstein and Galbally (2007) predicted that over a million C_{10} compounds (molecules with 10 carbon atoms) are likely to exist in the atmosphere, rendering the estimation of organic carbon fluxes between the ocean and the atmosphere impossible to resolve on a single compound basis. Hence, the focus on a few relevant volatile organic compounds, usually measured in marine ecosystems (Laturnus, 2001; Sinha et al., 2007), which account for a small fraction of the VOC and SOC compounds, do not allow a quantitative estimation of the air–water exchange of organic carbon exchanged at the ocean-atmosphere interphase.

There are numerous reports in the literature of studies demonstrating the production of single compounds or, at best, a modest set of individual VOC and SOC compounds by marine organisms, from macrolagae to phytoplankton (Laturnus et al., 2000; Bravo-Linares et al., 2007). These studies demonstrate that the production of exchangeable organic carbon is ubiquitous in the ocean (Giese et al., 1999). However, the quantification of the total amount of volatile organic carbon exchanged between the oceans and the atmosphere remains challenging. Anthropogenic SOCs are also found in the atmosphere worldwide and their exchange with the ocean is dominated by the diffusive fluxes from the gas-phase to the dissolved phase, while fluxes associated to aerosol dry deposition account for a small fraction of the total deposition (Jurado et al., 2008). However, there is neither an inventory of all anthropogenic SOC neither in the oceanic nor terrestrial atmosphere.

The problem, and the solution, is comparable to that of attempting to estimate the pool of dissolved organic carbon in the ocean from the sum of the concentrations of the individual compounds, with the operational solution being the development of the dissolved organic carbon concept and methods to collectively estimate the total pool of the compounds contributing to this pool in a single analysis (Spyres et al., 2000). Likewise, one pathway towards rendering the analysis of air–sea exchange of semi-volatile and volatile organic carbon was the development by Dachs et al. (2005) of concepts and procedures for total semi-volatile and volatile flux measurements. Dachs et al. (2005) proposed VOC and SOC compounds to be collectively measured as exchangeable dissolved organic carbon (EDOC), if measured in the water, or gaseous organic carbon (GOC), if measured in equilibrium with the atmosphere (Dachs et al., 2005; Ruiz-Halpern et al., 2010). The concepts of EDOC and GOC provide an approach comparable to that of conventional dissolved organic carbon (DOC) analysis to operationalize the quantification of these compounds (in $\mu\mathrm{mol\,C\,L^{-1}}$) beyond the limitations associated to approaches based on individual compounds (Dachs et al., 2005), which have not been resolved for the marine DOC pool either. EDOC and GOC are exchanged dynamically across the air–sea water interphase, a process that has been largely overlooked as it is currently missing from oceanic carbon budget assessments (IPCC fourth assessment (AR4) 2007). Yet, available studies identify the air–water exchange of organic carbon as an important component of the carbon budget of the subtropical NE Atlantic (Dachs et al., 2005) and subarctic fjords (Ruiz-Halpern et al., 2010), where these fluxes have been recently quantified. Indeed, as predicted by Jurado et al. (2008) these fluxes are comparable in order of magnitude to the fluxes of CO_2, and organic aerosols combined. Moreover, resolving EDOC is important because this is a component of DOC that is not captured with conventional measurements of DOC, which operationally measures non-purgeable organic carbon, as purgeable DOC, equivalent to EDOC, is removed from the pre-acidified sample along with DIC through the bubbling of the sample prior to DOC measurement involved in conventional marine DOC measurements (Spyres et al., 2000).

Polar ecosystems are characterized by intense biological activity. Thus, fluxes of exchangeable organic carbon are likely to be of regional, or even, global relevance. Indeed, Ruiz-Halpern et al. (2010) identified cold marine environments as areas potentially supporting large air–seawater organic carbon (OC) fluxes for a variety of reasons:

(1) Henry's law constant (H′) is low at low temperatures, displacing exchangeable OC to the water phase (Staudinger and Roberts, 2001); (2) polar macroalgae (Laturnus, 2001), and phytoplankton (Sinha et al., 2007) have already been identified as an important source of a wide variety of VOCs, including halogenated VOCs, methanol, acetone, acetaldehyde, DMS, and isoprene (Laturnus, 2001; Sinha et al., 2007); and (3) the increase in ice coverage in winter reduces the available area for these air–seawater OC exchanges, reducing their fluxes in winter and leading to a potential large release during summer ice melt (Ruiz-Halpern et al., 2010). Additionally, UV radiation, particularly high in the Antarctic spring and summer seasons (Madronich et al., 1998), may affect the stocks of exchangeable organic carbon in the water column by triggering phytoplankton cell death and lysis and the subsequent release of OC to the environment (Llabrés and Agustí, 2010), as well as through photochemical degradation of organic molecules, both in the water and the atmosphere (Zepp et al., 1998).

The Southern Ocean is particularly important in the regulation of the Earth's climate, as it acts as a significant sink for CO_2 (Sabine et al., 2004; Gruber et al., 2009) and connects the Pacific, Atlantic, and Indian oceans. Understanding the carbon budget in the Southern Ocean is, therefore, of particular interest. Unfortunately, whereas the air–sea fluxes of CO_2 have been evaluated extensively, there are no reported estimations of the air–sea fluxes of OC in the Southern Ocean as yet. Here we examine the pools of EDOC and GOC and the associated air–sea water exchanges of OC in the Antarctic Peninsula region, comparing these exchanges to the corresponding air–sea fluxes of CO_2. We estimate these parameters for the austral summers of years 2005, 2008, and 2009, from measurements taken during three cruises conducted along the Antarctic Peninsula, onboard R/V *Hespérides*.

2 Data set and methodology

2.1 Study site

Three cruises were conducted onboard the Spanish R/V *Hespérides* along the Antarctic Peninsula: ICEPOS (2 to 22 February 2005), ESASSI (5 to 16 January 2008) and ATOS-*Antarctica* (28 January to 23 February 2009). The ICEPOS and ATOS-*Antarctica* cruises followed similar trajectories around the Antarctic Peninsula. They covered the tip of the Antarctic Peninsula, from the Weddell Sea to the Bransfield Strait, and its western coast. The ESASSI cruise was restricted to the northern edge of the Weddell Sea, between the South Shetland and South Orkney Islands (Fig. 1).

2.2 Sampling

During the ICEPOS cruise, coupled measurements of EDOC in surface waters and GOC were taken at 61 locations, whereas only 20 and 25 coupled measurements were taken during the ESASSI and ATOS-*Antarctica* cruises, respectively. In addition to the coupled air–water measurements, depth profiles of EDOC concentration in the water column were performed during the ICEPOS and ATOS-*Antarctica* cruises. Additionally, several diel cycles and EDOC sampling at the surface microlayer (SML) were conducted during the ICEPOS cruise. Finally, measurements of CO_2 partial pressure were concurrently taken in air and seawater.

2.3 CO_2 measurements

Molar fraction of CO_2 in air (xCO_{2-a}) was measured continuously at 1 min intervals with a commercially available high precision (±1 ppm) non-dispersive infrared gas analyzer (EGM4, PP systems), passing clean air free of emissions from the vessel through an anhydrous calcium sulfate (Drierite) column to remove water vapor and avoid interferences in the detector. Seawater surface molar fraction of CO_2 (xCO_{2-w}) was measured by circulating water from a depth of 5 m, depth where the intake of the continuous flow-through system of the vessel is located. Water was pumped through a gas exchange column (1.25 × 9 membrane contactor, Celgard) and a closed-loop gas circuit fitted with an anhydrous calcium sulfate column circulated through the gas analyzer as above. The continuous flow of water and the small volume of air circulating counter-current through the gas exchange column ensured full and rapid equilibration between water and air (Calleja et al., 2005). Partial pressure of CO_2 in water and air corresponds to that in dry air (xCO_2). Then fugacity of CO_2in water (fCO_{2-w}) and air (fCO_{2-a}) are calculated by correcting for a 100 % water vapor pressure at 1 atm and by applying virial equation of state (Weiss, 1974). The analyzer was calibrated by using a commercial gas mixture of 541 ppm CO_2 and N_2.

2.4 DOC, EDOC and GOC H'^{-1} measurements

Water samples for the analysis of EDOC and DOC were collected by using Niskin bottles attached to a Rosette-CTD sampling system. For the analysis of DOC, duplicate samples were collected in 10 mL pre-combusted (4.5 h, 500 °C) glass ampoules filled directly with water from the Niskin bottle. They were acidified to a pH < 2 by adding 15 µL of concentrated (85 %) H_3PO_4, sealed under flame, and stored until analysis in the laboratory with a Shimadzu total organic carbon (TOC)-Vcsh analyzer, following standard non-purgeable organic carbon (NPOC) analysis (Spyres et al., 2000). Standards of 2 μmol C L^{-1} and 44 μmol C L^{-1} (provided by D. A. Hansell and W. Chen from the University of Miami) were used to assess the accuracy of our estimates. EDOC and GOC samples were collected following the procedure described by Dachs et al. (2005) and Ruiz-Halpern et al. (2010). Briefly, for GOC samples, filtered air (collected upstream from the boat to avoid contamination from in situ emissions) was bubbled for approximately 30 min in 50 mL of high purity free of carbon Mili-Q water acidified to a pH < 2 with concentrated (85 %) H_3PO_4. Defining the dimensionless Henry's Law constant (H') as the ratio of the concentrations in the gas phase and dissolved phase, this procedure allow estimation of the concentrations of organic carbon equilibrated with the gas-phase organic carbon (GOC H'^{-1}). EDOC measurements were obtained by bubbling 1 L of sampled water with high-grade (free of carbon) N_2 for 8 min, which we determined to suffice to reach equilibrium. The stream of gas with the evolved EDOC is redissolved in 50 mL of acidified, free of carbon Mili-Q water as for GOC H'^{-1}, Finally, EDOC and GOC H'^{-1} samples were stored in pre-combusted (4.5 h, 500 °C) glass ampoules, sealed under flame, until analysis in the laboratory as for DOC, but with the sparge gas procedure turned off in the Shimadzu total organic carbon (TOC)-Vcsh instrument (Dachs et al., 2005; Ruiz-Halpern et al., 2010). EDOC concentrations were corrected for contamination by subtraction following the analysis of blanks, obtained by directly bubbling the high purity acidified Mili-Q water with high-grade N_2 without the sample water after collection of each set of EDOC and GOC at the stations. Blank levels reflect the concentration of CO_2 equilibrated with water at the low temperatures of the southern ocean waters. The recoveries of the EDOC analysis was evaluated for acetone and were 31 % for the ICEPOS cruise. These values are lower than previously reported due to the low temperatures of seawater. However, since EDOC and GOC comprise thousands of compounds with different volatility, recoveries may be higher for compounds with higher values of the Henry's law constant.

2.5 Chlorophyll *a* (Chl *a*) and krill determination

Chl *a* concentration was determined spectrofluorimetrically (Parsons et al., 1984) for water samples collected from Niskin bottles at several depths. Chl *a* concentration was determined by filtering 50 mL samples onto 25 mm diameter Whatmann GF/F filters at each station. After filtration, filters were placed in tubes with a 90 % acetone solution for 24 h to extract the pigment. Chl *a* fluorescence was measured in a Shimadzu RF-5301 PC spectrofluorimeter, previously calibrated with a pure solution of Chl *a*.

Krill abundance was estimated by using a Simrad™ EK60 multifrequency echosounder. Working frequency was 38 kHz with a 256 µs sampling interval, 1024 µs pulse duration, and a bandwidth of 2425 Hz. The data obtained were processed by using SonarData Echoview 4 software. A maximum depth of 100 m and 80 dB of minimum target strength (TS), applying a time varied gain (TVG) function, was used to identify the krill targets. Finally, the data were subjected to a 100 m depth cell and a 1 min duration analysis. The number of targets detected down to 100 m cells was counted at 1 min intervals and the volume sampled by the beam calculated (Ruiz-Halpern et al., 2011).

2.6 Meteorological and seawater data

Pressure, wind speed (U_{10}), air temperature and solar radiation (from a Aanderaa meteorological station) and fluorescence, sea-surface temperature (SST), and salinity (Sal) (from a Seabird SBE 21 Thermo-salinographer) were continuously measured and averaged at 1 min intervals. Fluorescence was positively correlated with Chl *a* ($r = 0.74$, $p < 0.05$), allowing the use of fluorescence measurements as a proxy for phytoplankton abundance. Pitch, roll, and heading of the research vessel were also recorded at 1 min intervals and used in a routine embedded in the software, integrating navigation and meteorological data, to correct the wind speed data from the ship movement and flow distortion. The corrected wind velocities were then extrapolated to the wind velocity at 10 m (U_{10}) by using the following logarithmic expression: $U_{10} = U_z$ $[0.097\ln(z/10) + 1]^{-1}$, where z is the height of the wind sensor position (Hartman and Hammond, 1985).

2.7 Flux calculations

Diffusive air–sea water exchange of CO_2 was estimated by using the wind speed dependence of the mass transfer velocity (k_{600}) from instantaneous wind speeds (U_{10}, $\mathrm{m\,s^{-1}}$) following the expression $k_{600} = 0.222U_{10}^2 + 0.333U_{10}$ (Nightingale et al., 2000). The calculation of air–sea water CO_2 flux (F_{CO_2}) used the expression (Eq. 1):

$$F_{CO_2} = k_{600} \cdot S \cdot \Delta fCO_2 \qquad (1)$$

where $\Delta f\mathrm{CO_2}$ is the difference between $\mathrm{CO_2}$ fugacity in the surface of the ocean and that in the lower atmosphere ($\Delta f\mathrm{CO_2} = f\mathrm{CO_{2-w}} - f\mathrm{CO_{2-a}}$), k_{600} the gas transfer coefficient, normalized to a Schmidt number of 600, and S is the $\mathrm{CO_2}$ solubility term, calculated from sea water temperature and salinity (Weiss, 1974). Likewise, OC net diffusive fluxes (Faw) were estimated as the sum of gross volatilization ($\mathrm{Fvol} = k_0 \cdot \mathrm{EDOC}$) and absorption ($\mathrm{Fab} = -k_0 \cdot \mathrm{GOC\ H'^{-1}}$), where k_0 is the gas transfer velocity for exchangeable OC estimated from k_{600} values and Schmidt numbers assuming an average molecular weight (MW) of GOC of 120 g mol^{-1} and the same wind parameterization as for $\mathrm{CO_2}$. Details for the associated uncertainties derived from the use of an average MW are given in Ruiz-Halpern et al. (2010), and details on the direct measurement of GOC $\mathrm{H'^{-1}}$ are given in Dachs et al. (2005). The ICEPOS cruise delivered 61 coupled measurements of exchangeable organic carbon in water and air, whereas only 20 and 25 were obtained during ESASSI and ATOS-*Antarctica* cruises, respectively (Fig. 1). To characterize the stations sampled and to compare $\mathrm{CO_2}$ and exchangeable organic carbon fluxes, hourly averages of SST, Sal, (U_{10}), and $f\mathrm{CO_{2-w}}$, $f\mathrm{CO_{2-a}}$ and $F_{\mathrm{CO_2}}$ were calculated at the time EDOC and GOC $\mathrm{H'^{-1}}$ estimates were collected.

3 Results

3.1 Meteorological conditions and seawater column properties

The wind pattern was spatially variable, from lower velocities in sheltered areas to values higher than 20 m s^{-1} at some locations (Fig. 2a). Sea-surface temperature was close to 0 °C in the northeastern sector of the Antarctic Peninsula, close to the Antarctic Sound, and in the northern sector of the Weddell Sea, whereas higher values were observed in the western sector of the Antarctic Peninsula (Fig. 2b). The salinity pattern was less variable, the higher values were located to the north of the Antarctic Peninsula, between 60° W and 50° W, whereas the lower values were found in the western sector of the Antarctic Peninsula and eastern limb of the domain (Fig. 2c). Fluorescence showed maxima (indicator of phytoplankton blooms) at several locations close to the coastal margin of the Antarctic Peninsula (Fig. 2d).

Mean values for every area and cruise are shown in Table 1. In spite of the spatial variability, the mean wind speeds were quite constant among the areas and for the three cruises, ranging between 7 m s^{-1} in the western sector of the Antarctic Peninsula and 8 m s^{-1} in Bransfield Strait and Weddell Sea sector. Mean sea-surface temperature was close to 0 °C in the Weddell Sea sector of the sampled domain, but higher, around 1.5 °C, in the Bransfield Strait and western sector of the Antarctic Peninsula. However, the temperature range exceeded 4 °C as a minimum of −1.1 °C and a maximum temperature of 3.2 °C were recorded both in the Bellingsahusen Sea during the ATOS-*Antarctica* cruise. Salinities were less variable on average, the most saline sea-surface water was found during the ESASSI cruise, in the Weddell–Scotia Confluence (34.2), whereas the less saline was observed in the western sector of the Antarctic Peninsula (33.4). However, a maximum salinity of 34.43 in ICEPOS at the Bransfield strait and a minimum of 32.53 in the Bellingshausen Sea during ATOS-*Antarctica* were recorded.

3.2 Chlorophyll *a* and krill distribution

Table 1 also reports the mean values for biological parameters. Chl *a* concentrations ranged greatly (Fig. 2d), with differences of up to two orders of magnitude in Chl *a* concentration among stations (Table 1). The highest mean Chl *a* concentration (3.9 mg Chl *a* m^{-3}, Table 1) was found in the Weddell Sea during the ATOS-*Antarctica* cruise, while the lowest mean Chl *a* concentration was found in the Weddell–Scotia Confluence region during the ESASSI cruise (0.8 mg Chl *a* m^{-3}, Table 1). The lowest Chl *a* record was 0.12 mg Chl *a* m^{-3} in the Bellingshausen Sea during ATOS-*Antarctica* and an exceptionally high value of 31.66 mg Chl *a* m^{-3}, almost 300-fold the minimum value, was also measured during ATOS-*Antarctica*, but in the Weddell Sea (Table 1). Lower Krill densities were observed in the western sector of the Antarctic Peninsula and in the Weddell Sea side. Surprisingly, in the Bransfield Strait the mean concentration was twice the mean value of the neighboring areas. A maximum of 2.6×10^{-4} ind m^{-3} was found in the Bransfield strait during ICEPOS and a minimum of 1.9×10^{-5} ind m^{-3} in the Bellingshausen Sea during ATOS-*Antarctica*.

3.3 CO_2 concentration and fluxes

The fugacity of CO_2 in surface seawater was also highly variable with minima near shore, at the western sector of the Antarctic Peninsula, to the East of the tip of the Antarctic Peninsula, and near the South Orkney Islands (Fig. 3a). Concurrently, the partial pressures in the atmosphere, fCO_{2-a}, were less variable and displayed the opposite trend (Fig. 3b). The difference between both fugacities, ΔfCO_2, shows undersaturated areas along the coast of the Antarctic Peninsula, to the East of the peninsula, and next to the South Orkney Islands, whereas supersaturated areas were concentrated in the northern limb of the sampled domain and next to the South Shetland Islands (see Figs. 1 and 3d). The F_{CO_2} has a similar distribution than ΔfCO_2, except for a slight modulation due to the influence of wind speed in the flux calculations. This distribution supports oceanic CO_2 uptake along most of the sampled domain, the exceptions being the northern edge of the domain, the South Shetland Islands region, and several locations next to the Antarctic Peninsula that seem to act as a net source of CO_2 to the atmosphere (Fig. 3c).

Although the overall mean values of fCO_{2-w} and fCO_{2-a} were similar among cruises and regions, the horizontal distribution shows variability of fCO_{2-w} (see Table 2). At the sea surface, fCO_{2-w} ranges from strong supersaturation in the Bransfield Strait during ICEPOS to very strongly undersaturated in the Weddell Sea during the ATOS-Antartica cruise (Table 2). Supersaturation values above 400 µatm were found in all cruises and areas, while the Weddell Sea sector of the domain presented by far the most strongly undersaturated station (148 µatm), followed by a station located to the West of the Antarctic Peninsula (282 µatm). In the Bransfield Strait, minima values were close to equilibrium (350 µatm for fCO_{2-w} and the same value for fCO_{2-a}, see Table 2).

Regarding the net fluxes of CO_2 (F_{CO_2}, see Table 3), a maximum of 39 mmol C m^{-2} d^{-1}in the ocean uptake of carbon dioxide was found in the Weddell Sea sector during the ICEPOS cruise, while the maximum emission of CO_2 to the atmosphere (27 mmol C m^{-2} d^{-1}) was calculated also during the ICEPOS cruise but in the Bransfield Strait. Only in the western sector of the Antarctic Peninsula, there is dominance in the number of stations showing a net CO_2 uptake, while CO_2 emissions prevailed in the Weddell Sea sector of the sampled domain and in Bransfield Strait for all the cruises.

Although there were no strong correlations, fugacity of CO_2 in the surface layer of the water column was strongly undersaturated in sites with high Chl *a* concentrations and the sites more strongly supersaturated were those where the highest concentrations of Krill were measured (Fig. 4).

3.4 EDOC and GOC H'^{-1} distribution

Surface water EDOC, GOC H^{-1} and DOC were, on average, quite similar among cruises and regions (Table 2). However, the spatial variability of EDOC and GOC H'^{-1} was high, with similar coefficients of variation (C.V.) for EDOC and GOC H'^{-1} (388 % and 341 %, respectively, ranging from virtually no EDOC present in surface waters at some stations to a maximum of 147 µmol C L^{-1}; GOC H'^{-1} ranging between 9 µmol C L^{-1} and 137 µmol C L^{-1} among stations (Table 2). Despite this variability, around 60 % of both EDOC and GOC H'^{-1} concentrations were comprised between 10 and 50 µmol C L^{-1} (see Fig. 5). In contrast, DOC values were less variable, with a DOC mean value of 59 ± 4 µmol C L^{-1} (Table 2) and a C.V. of 37 %, with only two stations with values above 100 µmol C L^{-1}. The air–sea water exchange of OC (Faw, see Table 3) exceeded the net F_{CO_2} at many stations (Wilcoxon Sign-Rank test, $p < 0.05$), by as much as a factor of 10. Moreover, the air–sea water fluxes of CO_2 were not always in the same direction. There is a prevalence, though close to balance, of ocean uptake of gaseous organic carbon among cruises and areas, except for the Weddell

Sea sector where only 41 % of stations had net fluxes towards the ocean, and ESASSI stations which were in balance (50 %). In fact, the strongest sink for OC was found during the ESASSI cruise and reached 309 $\mathrm{mmol\,C\,m^{-2}\,d^{-1}}$, over the Weddell–Scotia Confluence region. The strongest OC emission from the ocean (710 $\mathrm{mmol\,C\,m^{-2}\,d^{-1}}$) was obtained in the Weddell Sea side during the ICEPOS cruise. These values of Faw are exceptionally high and are related to high wind events at the time of sampling. The flux of OC spanned a much broader range than that of CO_2, although two-thirds of the Faw values were situated in a narrow band, between −40 and 40 $\mathrm{mmol\,C\,m^{-1}\,d^{-1}}$ (Fig. 6), while all the fluxes of CO_2 at the sampled stations were located in this band. Two thirds of the values represented net emission of CO_2 to the atmopshere (Fig. 6). The Bransfield Strait presented a 100 % of supersaturated stations for $CO_2$and only in the western sector of the Antarctic Peninsula undersaturated stations did prevail over the supersaturated ones (Table 3).

EDOC was independent ($p > 0.05$) of $f\mathrm{CO}_{2-\mathrm{w}}$, SST or Sal, and no significant relationship was found between EDOC or Faw with Chl *a* or krill density ($p > 0.05$). There was no correspondence between EDOC and GOC H'^{-1} (Fig. 7), but during ICEPOS, EDOC values sampled in the surface microlayer (11 stations spanning along most of the cruise track) correlated linearly with EDOC concentrations – measured at 5 m depth ($R^2 = 0.55$, $p < 0.05$, Fig. 7).

3.5 Depth profiles and diel cycles

A total of 27 vertical profiles were performed, 5 during ICEPOS and 22 during ATOS-*Antarctica*. Figure 8 contains representative examples of depth profiles of EDOC and Chl *a* from two cruises showing 10 of these profiles an agreement between OC and Chl *a* (Fig. 8a and b); 4 profiles of OC showed an opposite pattern than that of Chl *a* (Fig. 8c); and 13 showed no clear pattern (Fig. 8d). A Pearson's chi-squared (X^2) analyses showed these profile relationships to be different than expected by chance ($X^2 = 15.5$, $p < 0.001$).

The diel cycles performed during ICEPOS, from 3 to 5 February, 13–14 February, and 16–18 February 2005, showed, in general, two distinct peaks around midday and midnight for EDOC, while GOC H'^{-1} showed no diel variability (Fig. 9).

4 Discussion

4.1 Water column an biological properties

The oceanographic properties of the Antarctic Peninsula depict this region as a highly dynamic and complex area, where several water masses with distinct characteristics are encountered (Mura et al., 1995). The cruises took place in the same season, albeit in different years. The ICEPOS and ATOS cruises followed similar tracks, whereas ESASSI took place a month earlier in austral summer of 2008 and was restricted to the Weddell–Scotia Confluence region (Fig. 1). Indeed, the mean and median values for the cruise data sets are remarkably similar for most of the properties shown in this study, particularly the physical characteristics at the air–sea surface interface. The western sector of the Antarctic Peninsula was, in general, warmer and less saline. At the time of sampling, some of the stations had an elevated content of Chl *a* and showed bloom conditions. This feature was also present close to the Antarctic Sound and close to the South Orkney Islands. These less saline waters are derived from the melting of the ice sheet during austral summer, as well as fresh water delivery form meltwater close to shore, and the accumulation of icebergs from the Weddell Sea in the South Orkney Islands, which has been shown to stimulate phytoplankton growth (Smith Jr. et al., 2007). Late spring and summer blooms are indeed controlled by abiotic factors as well as grazing pressure and are generally found in the marginal ice zone (Lancelot et al., 1993; Arrigo et al., 1998).

The large variability in Chl *a* concentrations, spanning two orders of magnitude, corroborates the patchy nature in the distribution of phytoplankton characteristic of Antarctic waters (Priddle et al., 1994). Krill density also displayed a patchy distribution, in agreement with previous observations (Murray, 1996), but the data presented here did not show any relationship between krill abundance and Chl *a* concentration, contrary to previous studies (Atkinson et al., 2004).

4.2 CO_2 fluxes

The spatial variability of CO_2 concentration in the sea surface layer was affected both by phytoplankton and krill abundance. These relationships were as expected: stations with the highest concentrations of Chl *a* supported the strongest undersaturation of CO_2; whereas stations were strongly supersaturated in CO_2 where krill abundance was highest. Indeed, Krill does not only consume phytoplankton, hence decreasing carbon fixation rates by algae, but it also remineralizes organic matter back to CO_2 through respiration (Mayzaud et al., 2005). However, the relationships between CO_2 and the spatial heterogeneity in Chl *a* and Krill were weak and driven by extremes. As CO_2 is a slow diffusing gas, these relationships are expected to be weak, since krill is highly mobile and the partial pressure of CO_2 would average out physical and biological processes over longer time scales not captured by the survey conducted here.

The fugacity of CO_2 in air, fCO_{2-a}, although less variable (approximately between 350 and 380 µatm, a range of less than 30 µatm, see Table 2), showed a distribution opposite to that of fCO_{2-w} (Fig. 3a and b). The direction and potential intensity of carbon dioxide flux is determined by the gradient between air and sea water fugacities, ΔfCO_2. Therefore, small scale, regional variability in atmospheric CO_2 can lead to variability in air–sea water fluxes. This possibility, however, needs additional research, since most global estimates of air–sea CO_2 fluxes are based on regional mean atmospheric CO_2 values (Takahashi et al., 1997, 2009). Wind speed, which has been postulated to have a larger effect in CO_2 fluxes in the coastal ocean (Nightingale et al., 2000), exerted a strong modulation in the intensity of observed air–sea CO_2 fluxes.

Hourly-averaged F_{CO_2} data point to a prevalence of net efflux of CO_2 to the atmosphere ($1.6 \pm 1.2\,\mathrm{mmol\,C\,m^{-2}\,d^{-1}}$), observed in 72 % of stations (Table 3, Fig. 5). However, the cruise track was not a random transit through the region, and therefore, the statistics of hourly-averaged do not necessarily represent the regional patterns. Indeed, mapping of F_{CO_2} data suggests marine waters around the Antarctic Peninsula to act as a moderate sink for CO_2 (Fig. 3c), in agreement with Gruber et al. (2009). The net emission to the atmosphere in this region comes then from several hotspots at specific locations of strong emissions of CO_2 to the atmosphere.

4.3 Organic carbon fluxes

Mean EDOC and GOC H'^{-1} values in this region (see Table 2) were remarkably consistent with the values observed in the mid Atlantic (mean 40 μmol C L^{-1}, range 10 to 115 μmol C L^{-1}; see Dachs et al., 2005), highlighting the ubiquotous nature of this pool of carbon. The DOC values found in our study, with an overall mean surface DOC of 59 ± 4 μmol C L^{-1} (Table 2) consistent with previous reports (e.g. Kähler et al., 1997), points to Antarctic surface waters as those supporting the lowest DOC pool in the ocean. Furthermore, in some cases DOC concentrations were lower than actual EDOC values. The low values of DOC render EDOC concentrations, comparable to those found in other areas (Dachs et al., 2005; Ruiz Halpern et al., 2010), proportionately more important in Antarctic waters. EDOC amounts, on average, to 67 % of the DOC present (Table 2); whereas in the mid Atlantic and subarctic regions EDOC amounts only to 30–40 % of DOC (Dachs et al., 2005; Ruiz-Halpern et al., 2010). Because the EDOC pool is not included in the conventional measurements of DOC, which represents the non-purgeable fraction of dissolved organic matter (Spyres et al., 2000), these results indicate that neglecting the EDOC pool may be a particularly important gap in understanding the carbon cycle in Antarctic waters. Indeed, EDOC could represent a potentially important source of carbon to fuel microbial processes, since microbial communities are often limited by carbon concentrations in these environments (e.g. Bird and Karl, 1999). However, experiments on the utilization of VOC and SOC in oceanic waters are still lacking and this hypothesis remains speculative.

The relationship reported for the subtropical Atlantic and subarctic regions (Dachs et al., 2005; Ruiz-Halpern et al., 2010) between atmospheric (GOC H'^{-1}) and dissolved exchangeable organic carbon (EDOC) was not seen in Antarctic waters (Fig. 7). This indicates that maybe other processes in the water column and the atmosphere, than simple equilibrium mixing between these two pools control the relative partitioning of EDOC and GOC H'^{-1}. Possible reasons to explain this weak relationship may come from more intense UV radiation in the Antarctic peninsula (Madronich et al., 1998), affecting some of the volatile species present in the atmosphere, by photochemical degradation (Zepp et al., 1998) and chemical reactions with OH^- radicals (Bunce et al., 1991), the degree of EDOC released by phytoplankton through UV induced cell lysis (Llabrés and Agustí, 2010) and subsequent photochemical degradation in the water column, or rapid bacterial usage of EDOC (Villaverde and Fernandez-Polanco, 1999). However, the positive relationship between 5 m depth EDOC and SML-EDOC (Fig. 8) provides support for a tight coupling between the processes occurring at 5 m depth and those occurring at the ocean surface microlayer, which is not always the case (Calleja et al., 2005), implying rapid diffusion of organic carbon gases at small spatial scales.

4.4 Depth profiles and diel cycles

The depth profiles of EDOC revealed the dynamic nature of this carbon pool (Fig. 8) and the participation of phytoplankton in the production of exchangeable organic carbon, consistent with its role as a source of DOC to the Antarctic marine environment (Ruiz-Halpern et al., 2011). Profiles also suggest active consumption in the water column where other components, such as bacteria, may consume EDOC, since bacteria are often limited by carbon supply in Antarctica, where the DOC pool is particularly small (Kähler et al., 1997). Moreover, antarctic krill has been recently demonstrated to release large amounts of DOC available to the microbial community (Ruiz-Halpern et al., 2011), and is likely to contribute to the EDOC pool as well, either mechanically, through sloppy feeding (Möller, 2007), or via direct excretion (Ruiz-Halpern et al., 2011).

The diel cycles performed provide further evidence of the dynamic nature of EDOC in the water column (Fig. 9). The relative invariance in the atmosphere of GOC H'^{-1} across the diel cycle suggests that it is EDOC, and its associated production and consumption dynamics, the determinant factor for the direction of the net organic carbon exchange and, under uniform wind speeds, for the variations in the magnitude of these fluxes. Peak EDOC concentrations were detected both at midday and middle of dark period. These cycles point to a progressive build up of EDOC in the water column as the day progresses: at midday, phytoplankton receives more light (both PAR and UV) and photosynthetic organic carbon production, and UV-induced damage accumulates; at midnight, the peak could possibly be related to Krill's vertical migration patterns, initialized by an upward motion at dusk (Zhou and Dorland, 2004) and subsequent release of EDOC by sloppy feeding and excretion (Møller, 2005), a hypothesis that awaits further experimental tests.

5 Conclusions

The flux of volatile OC was predominantly towards the ocean, as 57 % of the stations indicated an OC flux from the atmosphere toward the ocean (Table 3, Fig. 5), which corroborates previous reports of the ocean as a global sink for VOC and SOC (Dachs et al., 2005; Jurado et al., 2008; Ruiz-Halpern et al., 2010). However, a large portion (43 %) of the stations supported a net export of OC to the atmosphere, which has not been observed in the NE Subtropical Atlantic or Greenland Fjords, the other two areas where total VOC and SOC fluxes have been assessed (Dachs et al., 2005; Ruiz-Halpern et al., 2010). This dual source sink nature for VOC and SOC suggest that VOC and SOC are emitted in some parcels of water and absorbed in other, providing a pathway for the rapid redistribution and transport of organic carbon within the ocean supplementing that mediated by water mass transport (Dachs et al., 2005). Indeed, provided the lack of terrestrial sources of organic matter in the Southern Ocean, it is likely that organic matter is redistributed across the ocean through atmospheric transport from source areas to sink areas. For instance, penguin colonies are expected to be strong sources of volatile organic carbon that may enter the ocean downstream of wind trajectories. Although volatile organic carbon emissions from penguin colonies have not yet been assessed, penguin colonies have been found to be important sites of secondary emissions of volatile persisten organic pollutants (Roosens et al., 2007), with organic carbon likely to follow the same pathway. However, the origin of the organic carbon, possibly emitted from penguin colonies and other sites of intense biological activity, is marine. Moreover, the role of the atmosphere in the transport of marine organic carbon has not yet been addressed, but deserves further attention.

The data gathered during the three cruises in the Antarctic region provide compelling evidence for an important and dynamic role of volatile and semivolatile organic carbon in carbon cycling in the Southern Ocean, consistent with previous reports in the subtropical Atlantic (Dachs et al., 2005) and subarctic fjords (Ruiz-Halpern et al., 2010) as well as model calculations (Jurado et al., 2008).

EDOC pools in Antarctic marine waters may be comparatively more important than in other regions since it accounts for a larger proportion of total dissolved OC, with concentrations closely approaching to those of (non-purgeable) DOC. Air-sea water EDOC fluxes are also important, with the mean (±SE) ratio of the absolute air–sea OC flux to the absolute CO_2 across the study being 61 ± 30. Variability in these fluxes, however, resulted in air–sea water exchanges of organic carbon not too different from 0 when averaged across stations and cruises (Table 3), suggesting that emission and absorption of VOC and SOC represent pathways for transport and redistribution that are balanced across the region. Whereas emission and uptake of VOC and SOC compounds may be in approximate balance in this region, the individual compounds are probably not, as some components of this flux, such as persistent organic pollutants, are likely to move predominantly from the atmosphere to the ocean whereas some others, such as DMS, have oceanic sources and are expected to flow from the ocean to the atmosphere. Because the components of the flux originated in the ocean or the atmosphere are likely to have different properties, the flux remains significant even if, on a carbon basis, they are approximately in balance at the regional scale.

These results support previous reports (Dachs et al., 2005; Jurado et al., 2008; Ruiz-Halpern et al., 2010) highlighting that the understanding of the carbon budget of the ocean requires consideration of volatile and semivolatile organic carbon fluxes across the air–sea water interface. This net flux of organic carbon, comparable in magnitude to the flux of CO_2, is the result of a complex mixture of fluxes of different compounds. These compounds are also active in the atmosphere: the radiative balance through green house effects, the oxidative properties of the atmosphere, hydroxyl radical formation, ozone cycling and cloud and secondary aerosol formation. Likewise, little is known on the properties and possible effects of EDOC in the water column, and other possible producers other than micro and macroalgae. Indeed, bacteria can act as a source (Kuzma et al., 1995) or as a sink (Cleveland and Yavitt, 1998) of VOC as it has been demonstrated for the production and consumption of isoprene, and could contribute, not only to the EDOC pool in the water column, but also to its turnover. Moreover, the molecular weight of volatile and semivolatile species is low compared to that of DOC, and it is likely that these molecules can be taken up and metabolized by the microbial community possibly contributing to metabolic processes in the ocean.

In summary, the data presented here provide evidence of important air–sea fluxes of volatile and semivolatile species of organic carbon in the waters surrounding the Antarctic Peninsula, comparable in magnitude to air–sea CO_2 fluxes. Understanding the sources, sinks and cycling of volatile and semivolatile organic carbon is an imperative to understand the carbon budget of the ocean.

Acknowledgements. We thank the commander and crew of the RV *Hespérides* for dedicated and professional assistance, The personnel of the Unidad de Tecnología Marina (UTM) for highly professional technical support. Miquel Alcaráz for help with Krill collections, Pedro Echeveste for Chl *a* analysis and Amaya Álvarez-Ellacuría for her insight on matlab. This is a contribution to the Aportes Atmosféricos de Carbono Orgánico y Contaminanates al Óceano Polar (ATOS) and the spanish contribution to the Synoptic Shelf-Slope Interactions (ESASSI) funded by the Spanish ministry of Science under the scope of the International Polar Year (IPY).

References

Arrigo, K. R., Worthen, D., Schnell, A., and Lizotte. M. P.: Primary production in Southern Ocean waters, J. Geophys. Res., 103, 15587–15600, doi:10.1029/98JC00930, 1998.

Atkinson, A., Siegel, V., Pakhomov, E., and Rothery, P.: Long-term decline in krill stock and increase in salps within the Southern Ocean, Nature, 432, 100–103, doi:10.1038/nature02996, 2004.

Ayers, G. P. and Gillett, R. W.: DMS and its oxidation products in the remote marine atmosphere: implications for climate and atmospheric chemistry, J. Sea Res., 43, 275–286, 2000.

Bird, D. F. and Karl, D. M.: Uncoupling of bacteria and phytoplankton during the austral spring bloom in Gerlache Strait, Antarctic Peninsula, Aquat. Microb. Ecol., 19, 13–27, doi:10.3354/ame019013, 1999.

Bunce, N. J., Nakai, J. S., and Yawching, M.: A model for estimating the rate of chemical transformation of a VOC in the troposphere by two pathways: photolysis by sunlight and hydroxyl radical attack, Chemosphere, 22, 305–315, 1991.

Bravo-Linares, C. M., Mudge, S. M., and Loyola-Sepulveda, R. H.: Occurrence of volatile organic compounds (VOCs) in Liverpool Bay, Irish Sea, Mar. Pollut. Bull., 54, 1742–1753, doi:10.1016/j.marpolbul.2007.07.013, 2007.

Calleja, M. L., Duarte, C. M., Navarro, N., and Agustí, S.: Control of air–sea CO_2 disequilibria in the subtropical NE Atlantic by planktonic metabolism under the ocean skin, Geophys. Res. Lett., 32, L08606, doi:10.1029/2004GL022120, 2005.

Charlson, R. J., Lovelock, J. E., Andreae, M. O., and Warren, S. G.: Oceanic phytoplankton, atmospheric sulphur, cloud albedo and climate, Nature, 326, 655–661, 1987.

Cleveland, C. C. and Yavitt, J. B.: Microbial consumption of atmospheric isoprene in a temperate forest soil, Appl. Environ. Microb., 64, 172–177, 1998.

Dachs, J., Calleja, M. L., Duarte, C. M., Del Vento, S., Turpin, B., Polidori, A., Herndl, G. J., and Agustí, S.: High atmosphere-ocean exchange of organic carbon in the NE subtropical Atlantic, Geophys. Res. Lett., 32, L21807, doi:10.1029/2005GL023799, 2005.

Giese, B., Laturnus, F., Adams, F. C., and Wiencke, C.: Release of volatile iodinated C1–C4 hydrocarbons by marine macroalgae from various climate zones, Environ. Sci. Technol., 33, 2432–2439, doi:10.1021/es980731n, 1999.

del Giorgio, P. A. and Duarte, C. M.: Respiration in the open ocean, Nature, 420, 379–384, 2002.

Goldstein, A. H. and Galbally, I. E.: Known and unexplored organic constituents in the Earth's atmosphere, Environ. Sci. Technol., 41, 1514–1521, doi:10.1021/es072476p, 2007.

Gruber, N., Gloor, M., Fletcher, S. E. M., Doney, S. C., Dutkiewicz, S., Follows, M. J., Gerber, M., Jacobson, A. R., Joos, F., Lindsay, K., Menemenlis, D., Mouchet, A., Müller, S. A., Sarmiento, J. L., and Takahashi, T.: Oceanic sources, sinks, and transport of atmospheric CO_2, Global Biogeochem. Cy., 23, GB1005, doi:10.1029/2008GB003349, 2009.

Hartman, B. and Hammond. D. E.: Gas exchange in San Francisco Bay, Hydrobiologia, 129, 59–68, 1985.

Judd, A. G., Hovland, M., Dimitrov, L. I., García Gil, S., and Jukes, V.: The geological methane budget at continental margins and its influence on climate change, Geofluids, 2, 109–126, doi:10.1046/j.1468-8123.2002.00027.x, 2002.

Jurado, E., Dachs, J., Duarte, C. M., and Simó, R.: Atmospheric deposition of organic and black carbon to the global oceans, Atmos. Environ., 42, 7931–7939, 2008.

Kähler, P., Bjornsen, P. K., Lochte, K., and Antia, A.: Dissolved organic matter and its utilization by bacteria during spring in the Southern Ocean, Deep-Sea Res. Pt. II, 44, 341–353, doi:10.1016/S0967-0645(96)00071-9, 1997.

Kuzma, J., Nemecek-Marshall, M., Pollock, W. H., and Fall, R.: Bacteria produce the volatile hydrocarbon isoprene, Curr. Microbiol., 30, 97–103, 1995.

Lancelot, C., Mathot, S., Veth, C., and Baar, H.: Factors controlling phytoplankton ice-edge blooms in the marginal ice-zone of the northwestern Weddell Sea during sea ice retreat 1988: field observations and mathematical modeling, Polar Biol., 13, 377–387, doi:10.1007/BF01681979, 1993.

Laturnus, F.: Marine macroalgae in polar regions as natural sources for volatile organohalogens, Environ. Sci. Pollut. R., 8, 103–108, doi:10.1007/BF02987302, 2001.

Laturnus, F., Giese, B., Wiencke, C., and Adams, F. C.: Low-molecular-weight organoiodine and organobromine compounds released by polar macroalgae – the influence of abiotic factors, Fresen. J. Anal. Chem., 368, 297–302, doi:10.1007/s002160000491, 2000.

Llabrés, M. and Agustí, S.: Effects of ultraviolet radiation on growth, cell death and the standing stock of Antarctic phytoplankton, Aquat. Microb. Ecol., 59, 151–160, doi:10.3354/ame01392, 2010.

Madronich, S., McKenzie, R. L., Björn, L. O., and Caldwell, M. M.: Changes in biologically active ultraviolet radiation reaching the Earth's surface, J. Photoch. Photobio. B, 46, 5–19, 1998.

Mayzaud, P., Boutoute, M., Gasparini, S., Mousseau, L., and Lefevre, D.: Respiration in marine zooplankton: the other side of the coin: CO_2 production, Limnol. Oceanogr., 50, 291–298, 2005.

Møller, E. F.: Sloppy feeding in marine copepods: prey-size-dependent production of dissolved organic carbon, J. Plankton Res., 27, 27–35, 2005.

Møller, E. F.: Production of dissolved organic carbon by sloppy feeding in the copepods *Acartia tonsa*, *Centropages typicus*, and *Temora longicornis*, Limnol. Oceanogr., 52, 79–84, 2007.

Mura, M. P., Satta, M. P., and Agustí, S.: Water-mass influences on summer Antarctic phytoplankton biomass and community structure, Polar Biol., 15, 15–20, 1995.

Murray, A. W. A.: Comparison of geostatistical and random sample survey analyses of Antarctic krill acoustic data, ICES J. Mar. Sci., 53, 415–421, doi:10.1006/jmsc.1996.0058, 1996.

Nightingale, P. D., Malin, G., Law, C. S., Watson, A. J., Liss, P. S., Liddicoat, M. I., Boutin, J., and Upstill-Goddard, R. C.: In situ evaluation of air–sea gas exchange parameterizations using novel conservative and volatile tracers, Global Biogeochem. Cy., 14, 373–387, doi:10.1029/1999GB900091, 2000.

Parsons, T. R., Maita, Y., and Lalli, C. M.: A Manual of Chemical and Biological Methods for Seawater Analysis, Pergamon Press, Oxford, 1984.

Priddle, J., Brandini, F., Lipski, M., and Thorley, M. R.: Pattern and variability of phytoplankton biomass in the Antarctic Peninsula region: an assessment of the BIOMASS cruises, in: Southern Ocean Ecology: the BIOMASS Perspective, edited by: Sayed, S. Z., Cambridge University Press, Cambridge, 49–62, 1994.

Roosens, L., Van Den Brink, N., Riddle, M., Blust, R., Neels, H., and Covaci, A.: Penguin colonies as secondary sources of contamination with persistent organic pollutants, J. Environ. Monitor., 9, 822–825, doi:10.1039/B708103K, 2007.

Ruiz-Halpern, S., Sejr, M. K., Duarte, C. M., Krause-Jensen, D., Dalsgaard, T., Dachs, J., and Rysgaardd, S.: Air–water exchange and vertical profiles of organic carbon in a subarctic fjord, Limnol. Oceanogr., 55, 1733–1740, 2010.

Ruiz-Halpern, S., Duarte, C. M., Tovar-Sanchez, A., Pastor, M., Horstkotte, B., Lasternas, S., and Agustí, S.: Antarctic krill as a major source of dissolved organic carbon to the Antarctic ecosystem, Limnol. Oceanogr., 56, 521–528, doi:10.4319/lo.2011.56.2.0521, 2011.

Sabine, C. L., Feely, R. A., Gruber, N., Key, R. M., Lee, K., Bullister, J. L., Wanninkhof, R., Wong, C. S., Wallace, D. W. R., Tilbrook, B., Millero, F. J., Peng, T. H., Kzyr, A., Ono, T., and Rioas, A. I.: The oceanic sink for anthropogenic CO_2, Science, 305, 367–371, doi:10.1126/science.1097403, 2004.

Siedler, G., Church, J., and Gould, J., and Griffies, S.: Ocean Circulation and Climate: Observing and Modelling the Global Ocean, Academic Press, San Diego, USA, 2001.

Sinha, V., Williams, J., Meyerhöfer, M., Riebesell, U., Paulino, A. I., and Larsen, A.: Air-sea fluxes of methanol, acetone, acetaldehyde, isoprene and DMS from a Norwegian fjord following a phytoplankton bloom in a mesocosm experiment, Atmos. Chem. Phys., 7, 739–755, doi:10.5194/acp-7-739-2007, 2007.

Smith Jr., K. L., Robison, B. H., Helly, J. J., Kaufmann, R. S., Ruhl, H. A., Shaw, T. J., Twining, B. S., and Vernet, M.: Free-drifting icebergs: hot spots of chemical and biological enrichment in the Weddell Sea, Science, 317, 478–482, doi:10.1126/science.1142834, 2007.

Spyres, G., Nimmo, M., Worsfold, P. J., Achterberg, E. P., and Miller, A. E. J.: Determination of dissolved organic carbon in seawater using high temperature catalytic oxidation techniques, TRAC-Trend. Anal. Chem., 19, 498–506, 2000.

Solomon, S., Qin, D., Manning, M., Chen, Z., Marquis, M., Averyt, K. B., Tignor, M., and Miller, H. L.: Climate Change 2007 – The Physical Science Basis: Contribution of Working Group I to the Fourth Assessment Report of the IPCC, Cambridge University Press, Cambridge, UK, 2007.

Staudinger, J. and Roberts, P. V.: A critical compilation of Henry's law constant temperature dependence relations for organic compounds in dilute aqueous solutions, Chemosphere, 44, 561–576, 2001.

Takahashi, T., Feely, R. A., Weiss, R. F., Wanninkhof, R. H., Chipman, D. W., Sutherland, S. C., and Takahashi, T. T.: Global air–sea flux of CO_2: an estimate based on measurements of sea–air pCO_2 difference, P. Natl. Acad. Sci. USA, 94, 8292–8299, 1997.

Takahashi, T., Sutherland, S. C., Wanninkhof, R., Sweeney, C., Feely, R. A., Chipman, D. W., Hales, B., Friederich, G., Chavez, F., Sabine, C., Watson, A., Bakker, D. C. E., Schuster, U., Metzl, N., Yoshikawa-Inoue, H., Ishii, M., Midorikawa, T., Nojiri, Y., Körtzinger, A., Steinhoff, T., Hoppema, M., Olafsson, J., Arnarson, T. S., Tilbrook, B., Johannessen, T., Olsen, A., Bellerby, R., Wong, C. S., Delille, B., Bates, N. R., and de Baar. H. J. W.: Climatological mean and decadal change in surface ocean pCO_2, and net sea-air CO_2 flux over the global oceans, Deep-Sea Res. Pt. II, 56, 554–577, doi:10.1016/j.dsr2.2008.12.009, 2009.

Villaverde, S. and Fernandez-Polanco, F.: Spatial distribution of respiratory activity in *Pseudomonas putida* 54G biofilms degrading volatile organic compounds (VOC), Appl. Microbiol. Biot., 51, 382–387, doi:10.1007/s002530051406, 1999.

Weiss, R. F.: Carbon dioxide in water and seawater: the solubility of a non-ideal gas, Mar. Chem., 2, 203–215, doi:10.1016/0304-4203(74)90015-2, 1974.

Zepp, R. G., Callaghan, T. V., and Erickson, D. J.: Effects of enhanced solar ultraviolet radiation on biogeochemical cycles, J. Photochem. Photobio. B, 46, 69–82, doi:10.1016/S1011-1344(98)00186-9, 1998.

Zhou, M. and Dorland, R. D.: Aggregation and vertical migration behavior of *Euphausia superba*, Deep-Sea Res. Pt. II, 51, 2119–2137, doi:10.1016/j.dsr2.2004.07.009, 2004.

Table 1. Mean ± standard error (SE), median and ranges for the physical and biological parameters measured at the stations where coupled EDOC-GOC measurements were taken. Data for all three cruises; ICEPOS in 2005, ESASSI in 2008, and ATOS-*Antarctica* in 2009. Data were grouped into cruises and areas. Note that means for the different areas were estimated from the three cruises. There was no acoustic data to estimate krill density for the ESASSI cruise.

Surface	SST °C	Sal	U m s^{-1}	Chl *a* mg m^{-3}	Krill density 10^{-6} ind m^{-3}
Cruise					
ICEPOS	1.40 ± 0.09 1.70 [(−0.4)–(+2.1)]	33.70 ± 0.05 33.80 [32.7–34.4]	8.2 ± 0.5 8.6 [0.5–16.9]	2.4 ± 0.3 2.2 [0.5–4.6]	85 ± 8 72 [27–260]
ESASSI	0.32 ± 0.13 0.25 [(−0.5)–(+1.5)]	34.21 ± 0.04 34.28 [33.75–34.38]	7.4 ± 0.7 7.4 [1.7–11.9]	0.8 ± 0.1 0.85 [0.17–1.27]	no data
ATOS	1.30 ± 0.20 1.62 [(−1.1)–(+3.18)]	33.80 ± 0.09 33.80 [32.5–34.33]	6.6 ± 0.5 6 [2.7–11.6]	3.9 ± 1.4 1.68 [0.11–31.6]	66 ± 6 62 [19–160]
Area					
Weddell Sea sector	0.09 ± 0.08 0.02 [(−0.47)–(+0.96)]	34.12 ± 0.05 33.81 [32.74–34.43]	8.1 ± 0.6 7.8 [1.7–13.3]	3.6 ± 1.6 2.2 [0.5–4.6]	59 ± 7 72 [27–260]
Bransfield strait	1.61 ± 0.09 1.75 [(−0.17)–(+2.76)]	33.98 ± 0.03 33.90 [33.70–34.40]]	8.1 ± 0.6 8.2 [0.5–16.9]	2.6 ± 0.4 2.41 [0.33–7.7]	110 ± 11 81 [20–260]
Western sector of the Antarctic Peninsula	1.50 ± 0.80 1.72 [(−1.1)–(+3.18)]	33.40 ± 0.30 33.40 [32.50–33.80]	7.0 ± 3.0 6.3 [2.4–12.7]	1.7 ± 0.7 1.16 [0.12–4.55]	60 ± 50 56 [19–160]

Title Page
Abstract Introduction
Conclusions References
Tables Figures
◀◀ ▶▶
◀ ▶
Back Close
Full Screen / Esc
Printer-friendly Version
Interactive Discussion

Table 2. Mean ± standard error (SE), median and ranges for CO_2 fugacity in water and air, EDOC, GOC H'^{-1} and DOC throughout the track of the three cruises, ICEPOS in 2005, ESASSI in 2008, and ATOS-*Antarctica* in 2009. Data were grouped into cruises and basins. Note that means for the different areas come from all three cruises, and that there is no DOC data for the ESASSI cruise.

Surface	fCO_{2-w} µatm	fCO_{2-a} µatm	EDOC $\mu mol\,C\,L^{-1}$	GOC H'^{-1} $\mu mol\,C\,L^{-1}$	DOC $\mu mol\,C\,L^{-1}$
Cruise					
ICEPOS	368 ± 10	356 ± 1	36 ± 4	35 ± 3	54 ± 1
	374 (183–475)	357 (345–374)	27 (0–147)	29 (11–134)	54 (45–63)
ESASSI	396 ± 8	357 ± 1.4	40 ± 8	43 ± 9	no data
	400 (271–440)	358 (345–366)	31 (0–125)	34 (9–136)	
ATOS	341 ± 13	367 ± 1.4	60 ± 5	73 ± 5	62 ± 7
	364 (148–416)	367 (350–379)	57 (1–102)	70 (16–104)	54 (45–181)
Area					
Weddell Sea sector	346 ± 16	360 ± 1.4	49 ± 7	40 ± 5	71 ± 16
	387 (148–440)	360 (345–376)	42 (0–147)	30 (9–137)	56 (48.15–118.37)
Bransfield strait	401 ± 6	360 ± 1.0	39 ± 5	50 ± 4	54 ± 1
	389 (350–475)	359 (350–379)	34 (1–102)	44 (20–134)	53 (45–66)
Western sector of the	344 ± 7	356 ± 1.4	41 ± 6	47 ± 8	58 ± 5
Antarctic Peninsula	351 (282–419)	353 (346–372)	21 (0–98)	21 (11–100)	54 (45–107)
Total Mean ± SE	367 ± 7	359 ± 0.8	43 ± 3	46 ± 3	59 ± 4

Table 3. Mean ± standard error (SE), median and ranges for fluxes of organic carbon (Fvol, gross volatilization; Fab, gross absorption; Faw, net OC air–sea water exchange), and CO_2 (F_{CO_2}) throughout the track of the three cruises, ICEPOS in 2005, ESASSI in 2008, and ATOS-*Antarctica* in 2009. Data were grouped into cruises and areas. The percentage of stations with undersaturated CO_2, and OC uptake by the ocean are also shown.

Surface	Fvol mmol C m^{-2} d^{-1}	Fab mmol C m^{-2} d^{-1}	Faw mmol C m^{-2} d^{-1}	F_{CO_2} mmol C m^{-2} d^{-1}	CO_2 uptake % stations	OC uptake % stations
Cruise						
ICEPOS	100 ± 18	−90 ± 11	10 ± 17	1.0 ± 2.0	20	56
	48 (0–820)	−70 [−360–(0)]	−7 [−232–(+709)]	2.3 [−39–(+27)]		
ESASSI	100 ± 30	−120 ± 40	−20 ± 20	6.4 ± 1.6	10	50
	35 (0.6–556)	−33 [−606–(0)]	3 [−310–(+101)]	4.1 [−5–(+21)]		
ATOS	100 ± 20	−130 ± 20	−27 ± 11	−2.0 ± 1.4	46	71
	72 (1–385)	−88 [−457–(−24)]	−15 [−161–(+63)]	0.05 [−20–(+13)]		
Area						
Weddell Sea sector	140 ± 40	−120 ± 30	20 ± 30	−2.0 ± 3.0	38	41
	72 (0.6–820)	−56 [−606–(0)]	6 [−310–(+710)]	1.2 [(−38.7)–(+20.6)]		
Bransfield strait	103 ± 17	−129 ± 16	−27 ± 12	6.9 ± 1.2	0	72
	80 (0–457)	−109 [−457–(0)]	−18 [−232–(+224)]	4.26 (0–27.4)		
Western sector of the Antarctic Peninsula	66 ± 13	−64 ± 13	2.24 ± 12	−1.5 ± 0.8	56	52
	41 (0–293)	−45 [−386–(0)]	−441 [−161–(+150)]	−1.7 [−8.9–(+6.3)]		
Total Mean ± s.e	107 ± 13	−110 ± 11	−2.17 ± 11	1.6 ± 1.2	28 ± 10	57 ± 5

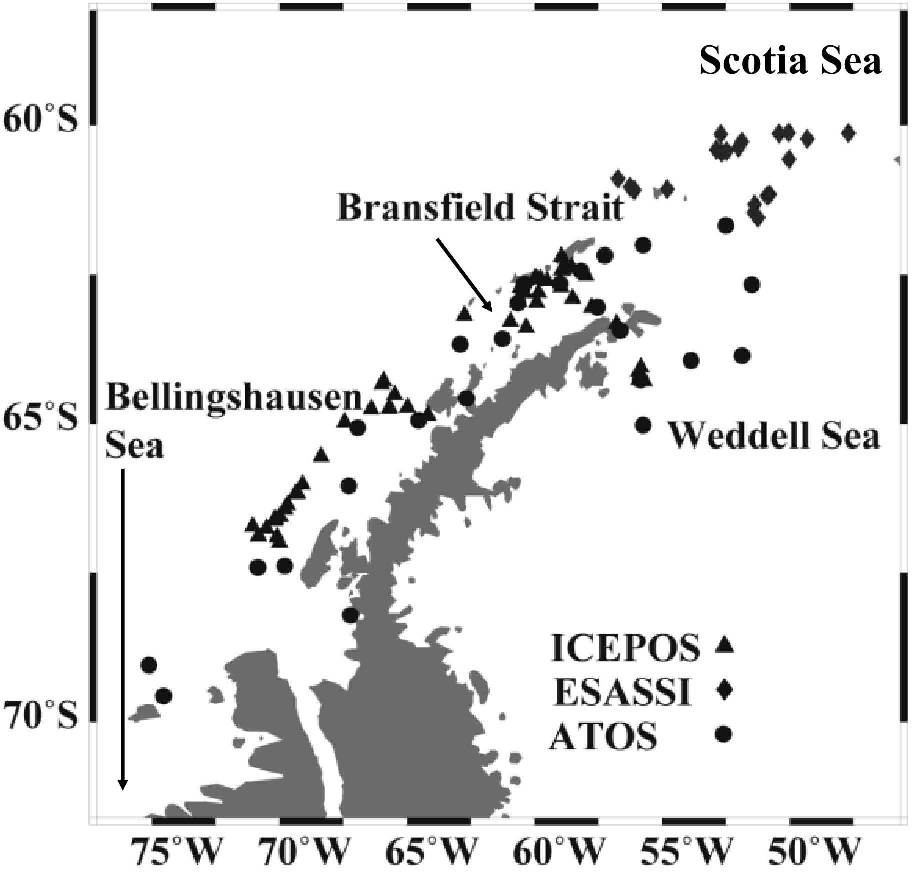

Fig. 1. Map of the region and the stations sampled during the three cruises: ICEPOS (triangles); ESASSI (diamonds); ATOS-*Antarctica* (circles).

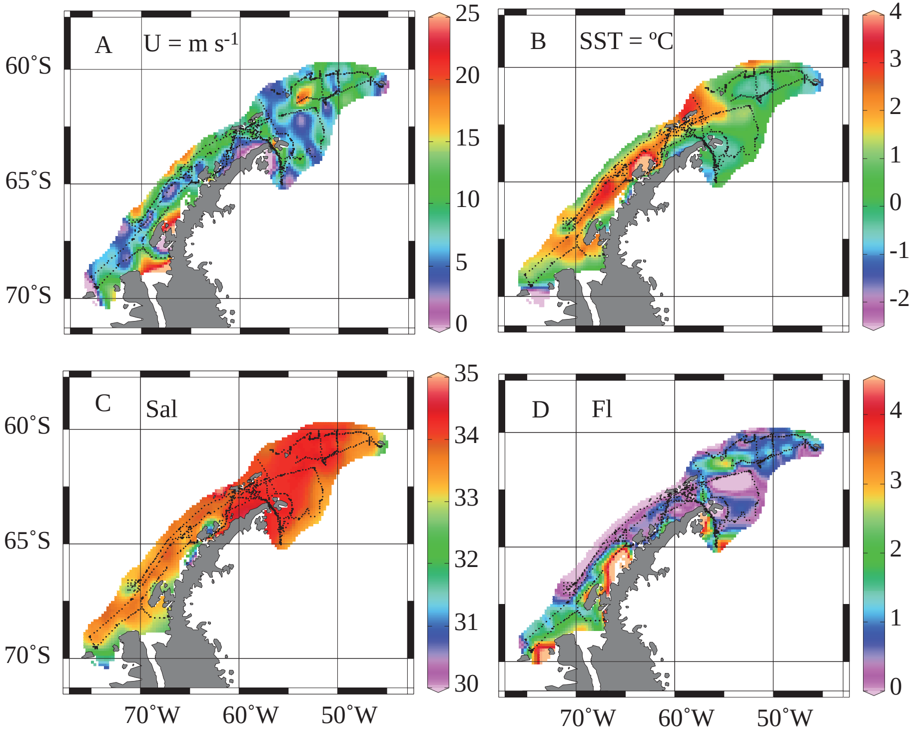

Fig. 2. The distribution of shipboard continuous measurements of windspeed (U, $\mathrm{m\,s^{-1}}$, **A**), sea-surface temperature (SST, ˚C, **B**), salinity (Sal, **C**), and fluorescence (Fl, **D**).

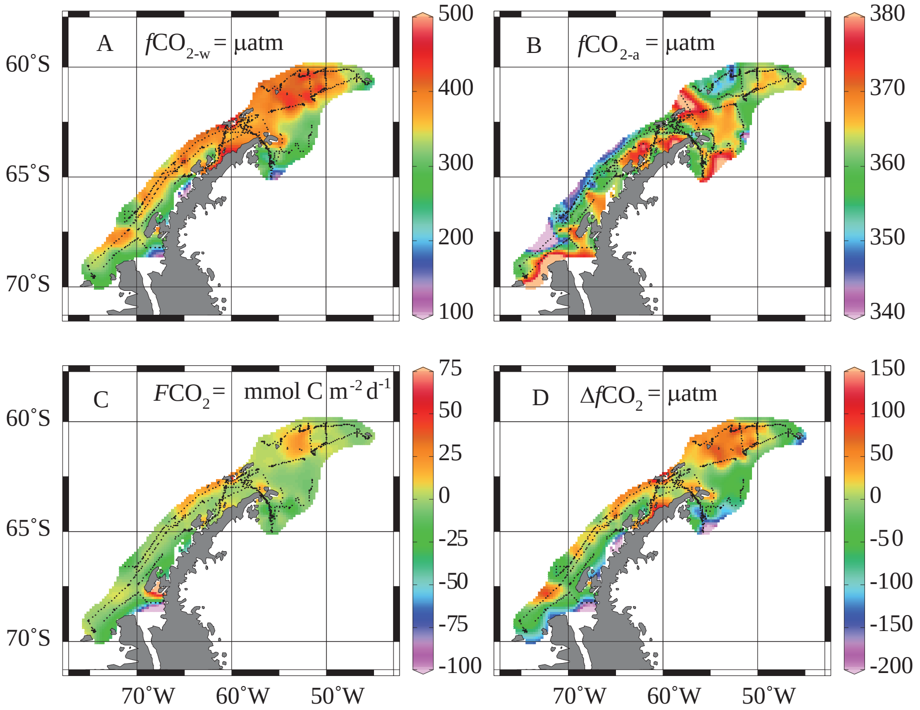

Fig. 3. The distribution of shipboard continuous measurements of fCO_{2-w} (µatm, **A**), fCO_{2-a} (µatm, **B**), F_{CO_2}(mmol C m^{-2} d^{-1}, **C**), and ΔfCO_2 (µatm, **D**).

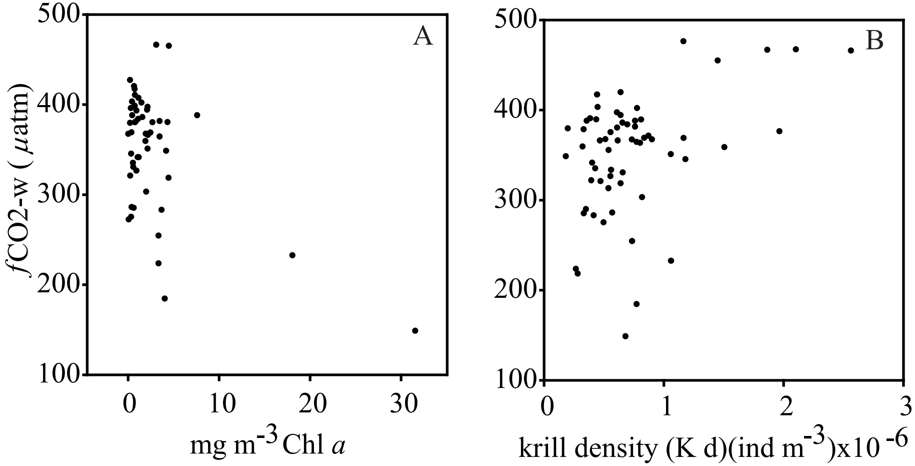

Fig. 4. Scatterplots of $f\text{CO}_{2-\text{w}}$ vs Chl *a* **(A)** and Krill density **(B)**. Data combined for all cruises and stations.

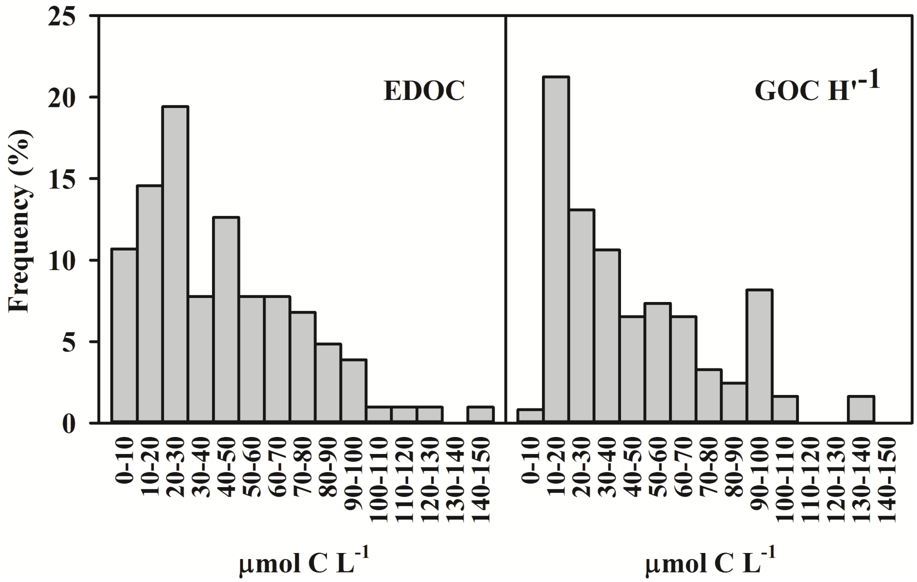

Fig. 5. Frequency distribution of surface EDOC and GOC H$'^{-1}$ (µmol C L^{-1}) for all three cruises.

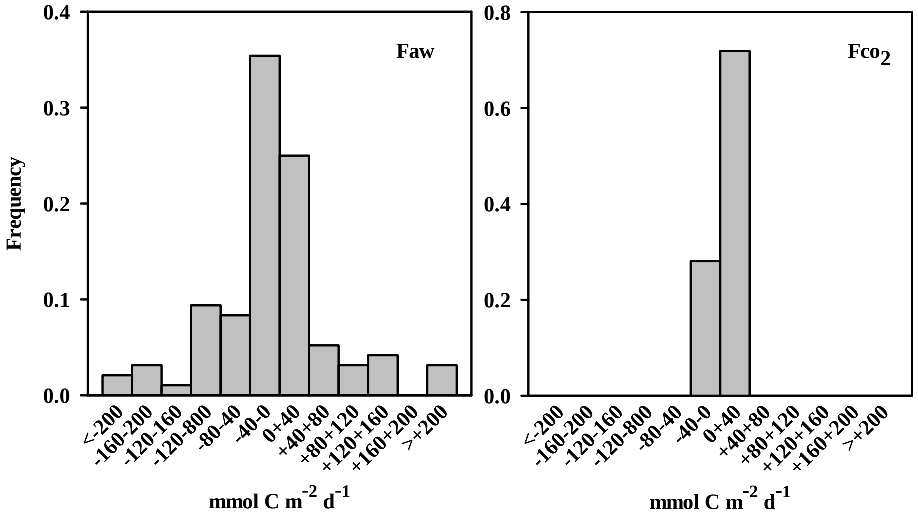

Fig. 6. Frequency distribution of air–sea fluxes of exchangeable organic carbon (Faw) and F_{CO_2} (mmol m^{-2} d^{-1}).

BGD

10, 16173–16211, 2013

Ocean-atmosphere exchange of organic carbon and CO_2

S. Ruiz-Halpern et al.

Title Page
Abstract
Introduction
Conclusions
References
Tables
Figures
◀|
|▶
◀
▶
Back
Close
Full Screen / Esc
Printer-friendly Version
Interactive Discussion

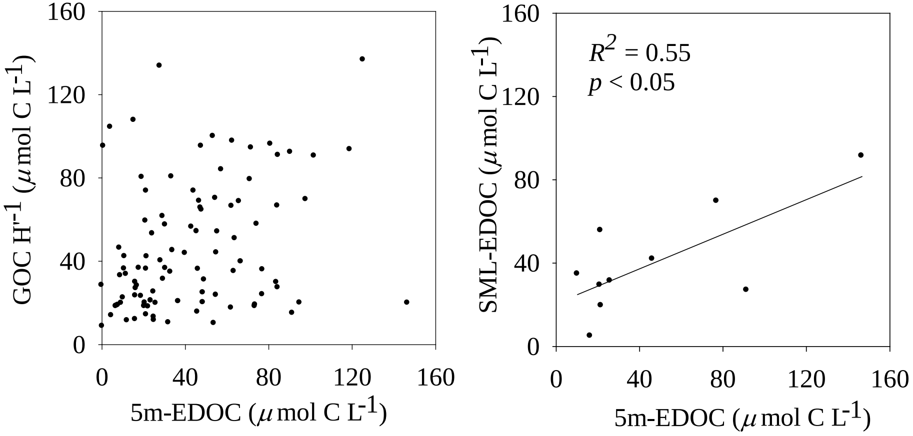

Fig. 7. Relationship between GOC H'^{-1} and EDOC at 5 m depth and the relationship between EDOC in the surface microlayer (SML-EDOC) and EDOC at 5 m depth. The solid line shows the fitted regression equation (GOC $H'^{-1} = 20.9 + 0.42$ EDOC, $R^2 = 0.55$; $p < 0.05$). Data for 11 stations during the ICEPOS cruise.

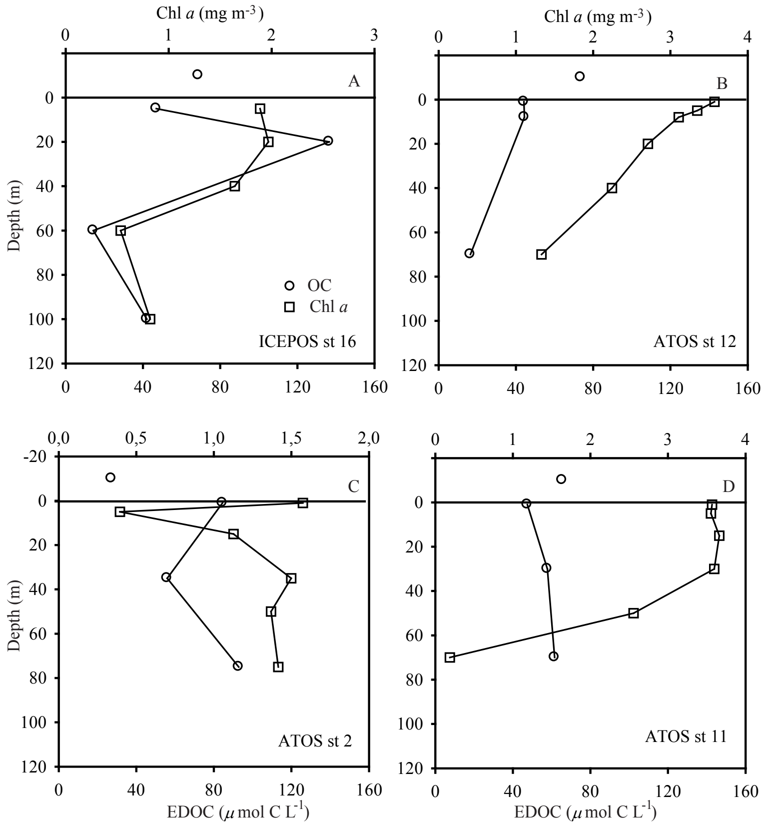

Fig. 8. Representative depth profiles of EDOC and Chl *a*. Example profile performed during ICEPOS **(A)**. During ATOS-*Antarctica*, 9 followed Chl *a* **(B)**, 10 showed no clear pattern **(C)**, and 3 were opposite to Chl *a* **(D)**. Open circles refer to organic carbon (OC) measured as EDOC in the water, and as GOC H'^{-1}(single open circle) in the atmosphere, open squares (Chl *a*).

BGD

10, 16173–16211, 2013

Ocean-atmosphere exchange of organic carbon and CO_2

S. Ruiz-Halpern et al.

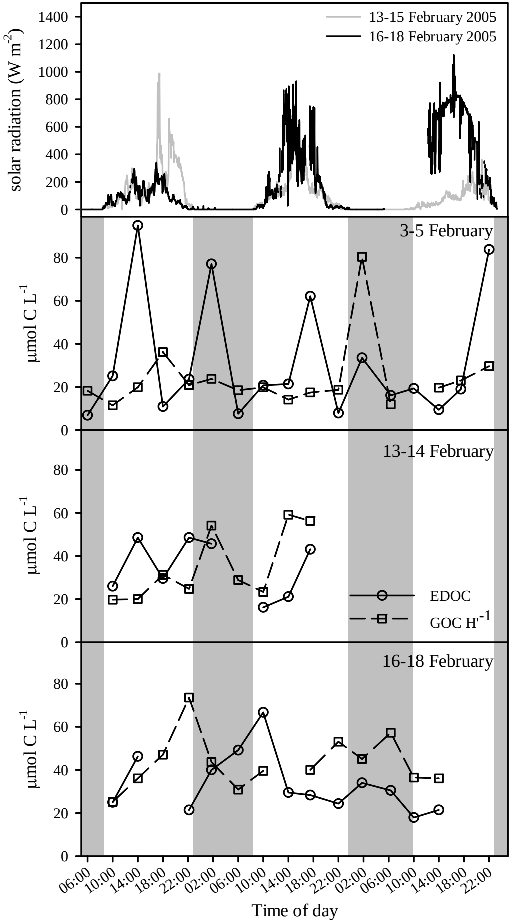

Fig. 9. Diel variability of EDOC (solid line, open circles) and GOC H'^{-1} (dashed line, open squares). The top panel shows solar radiation for the different days sampled, data for the 3–5 February cycle is missing due to equipment failure.